Electronic Supplementary Information for

Novel hybrid benzoazacrown ligand as chelator for Lead and Copper cations: what the difference a pyridine makes

by B.V. Egorova, L.S. Zamurueva, A.D. Zubenko, A.V. Pashanova, A.A. Mitrofanov, A.B. Priselkova, Yu.V. Fedorov, A.L. Trigub, O.A. Fedorova and S.N. Kalmykov

Content

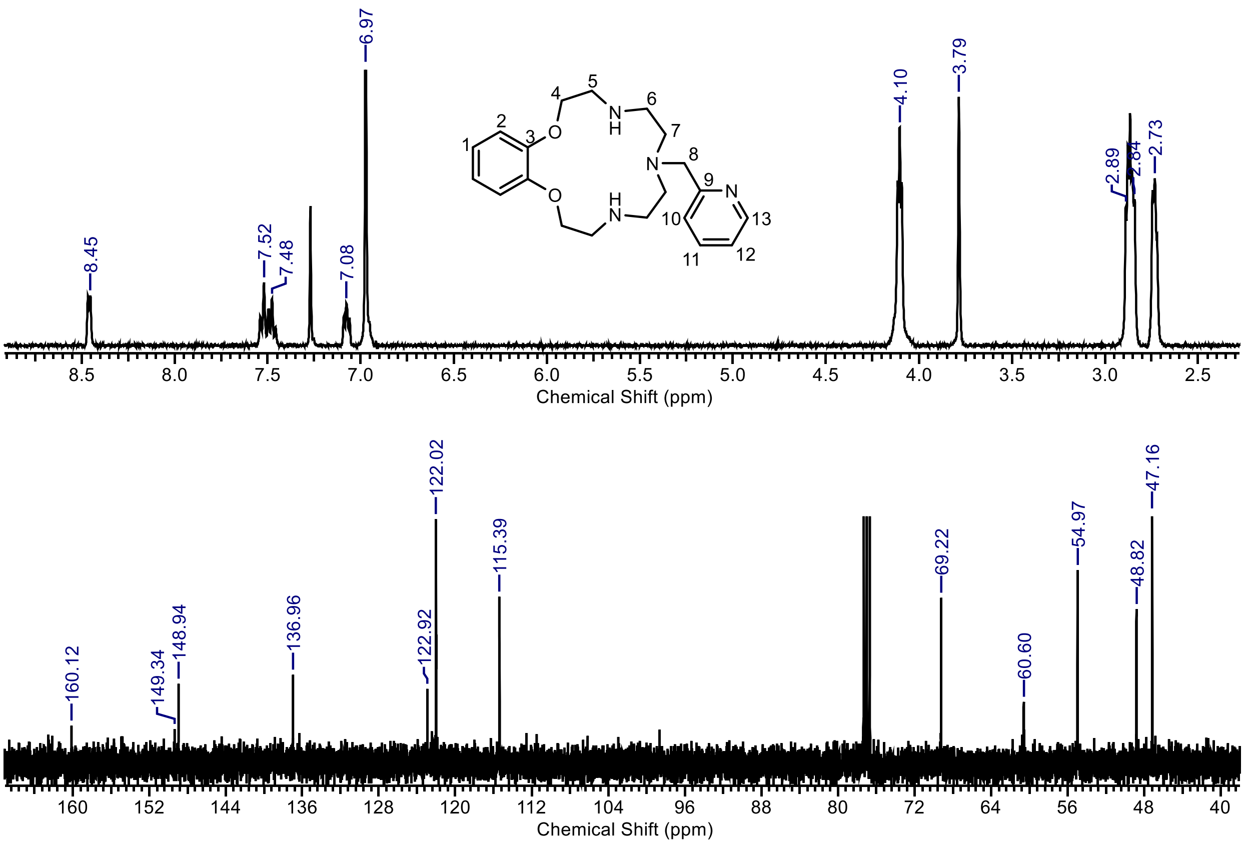

Figure S1. ^{1}H and ^{13}C NMR spectra of **3** in $CDCl_3$.

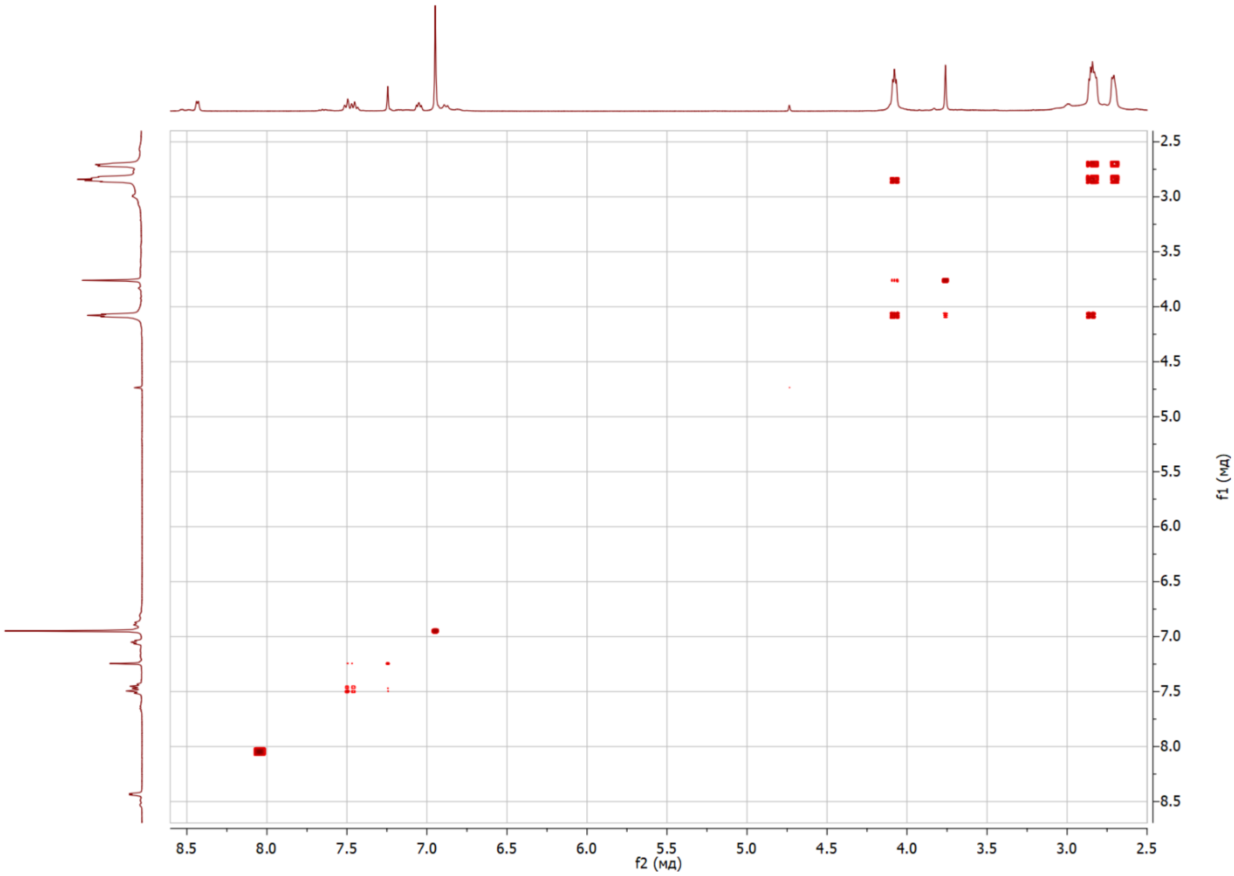

Figure S2. COSY spectrum of **3** in $CDCl_3$.

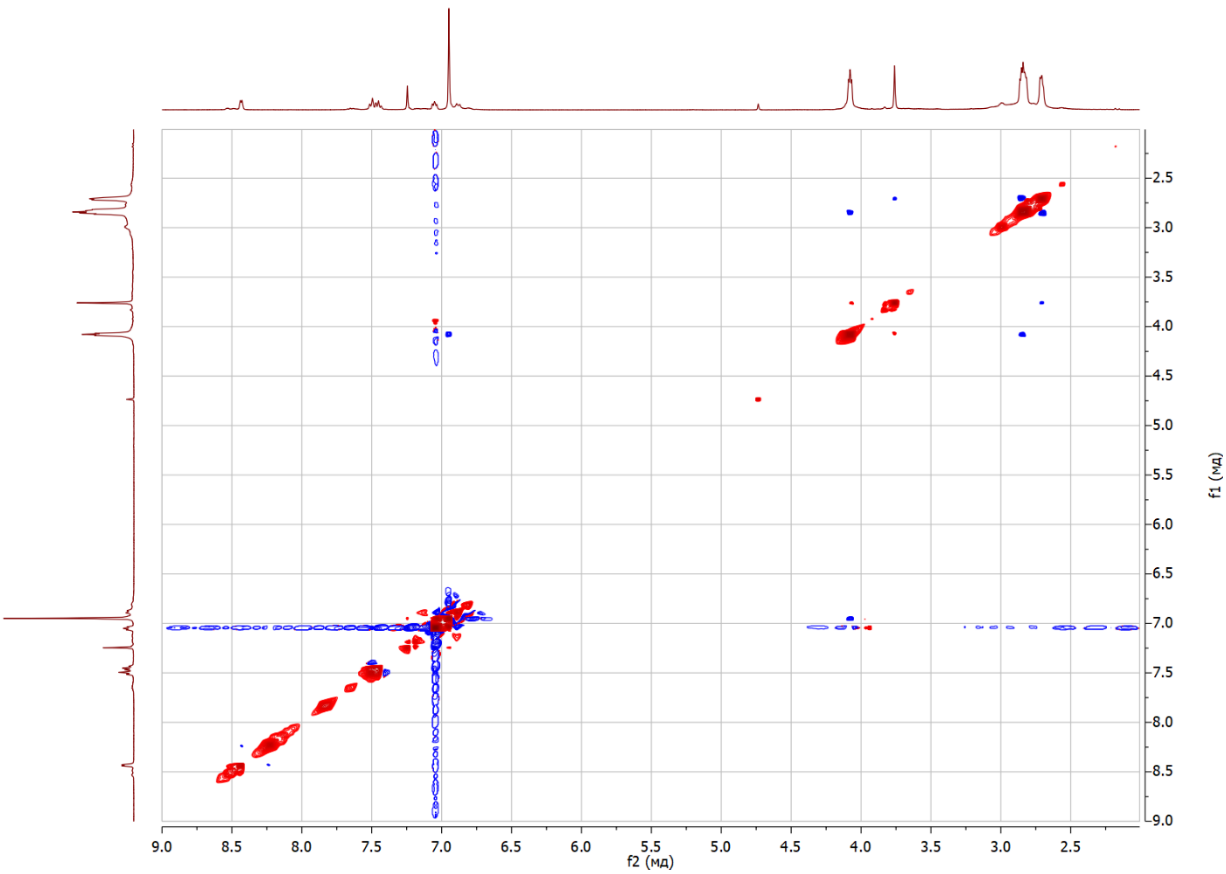

Figure S3. NOESY spectrum of **3** in $CDCl_3$.

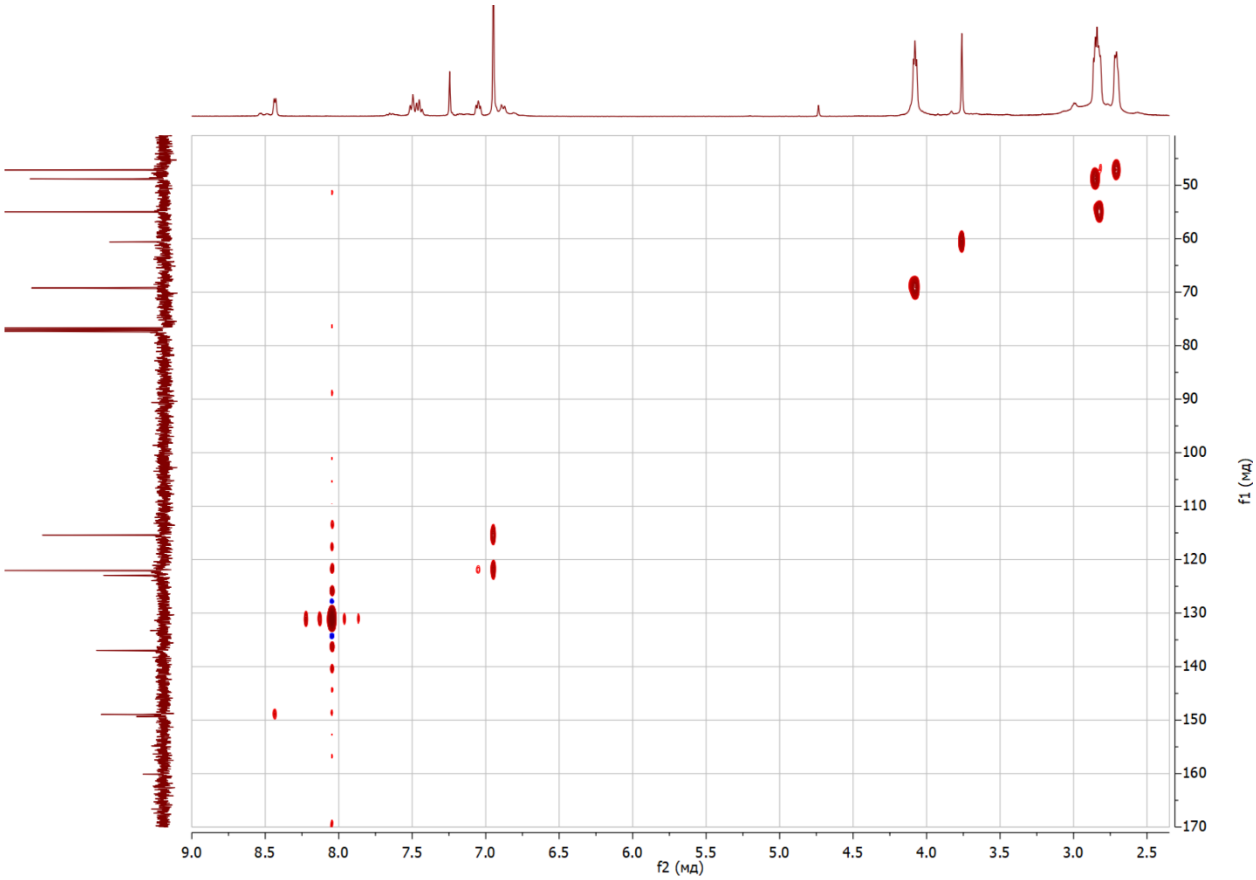

Figure S4. HSQC spectrum of **3** in $CDCl_3$.

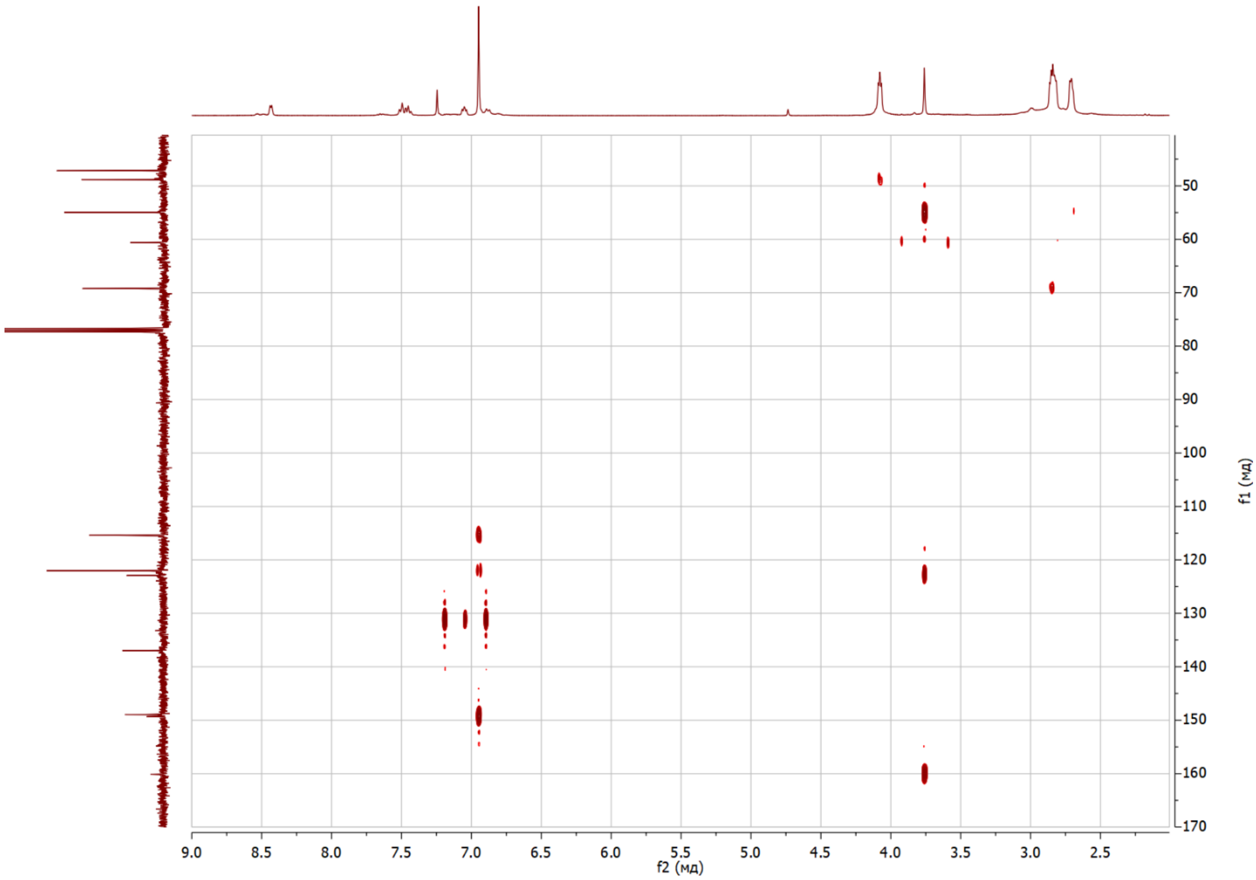

Figure S5. HMBC spectrum of **3** in $CDCl_3$.

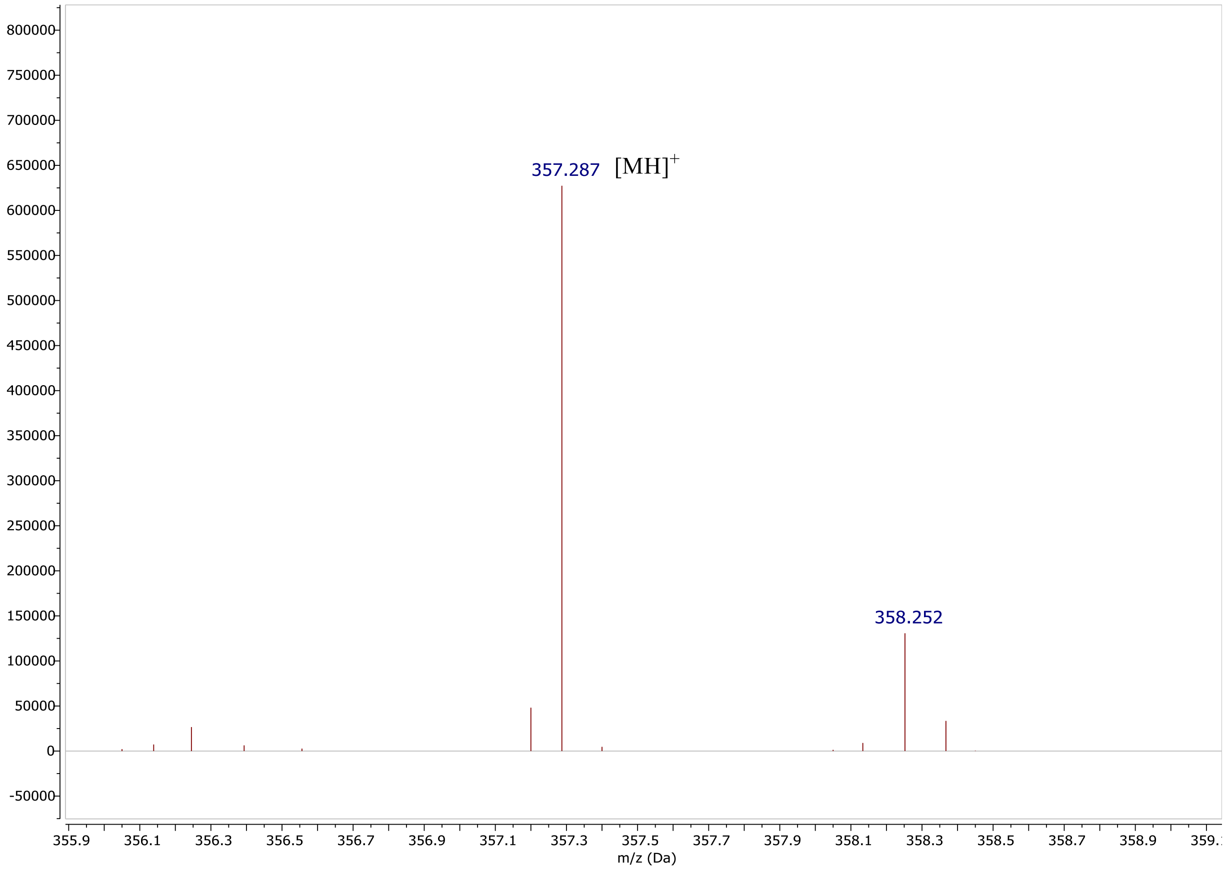

Figure S6. MS (ESI) spectrum of 3.

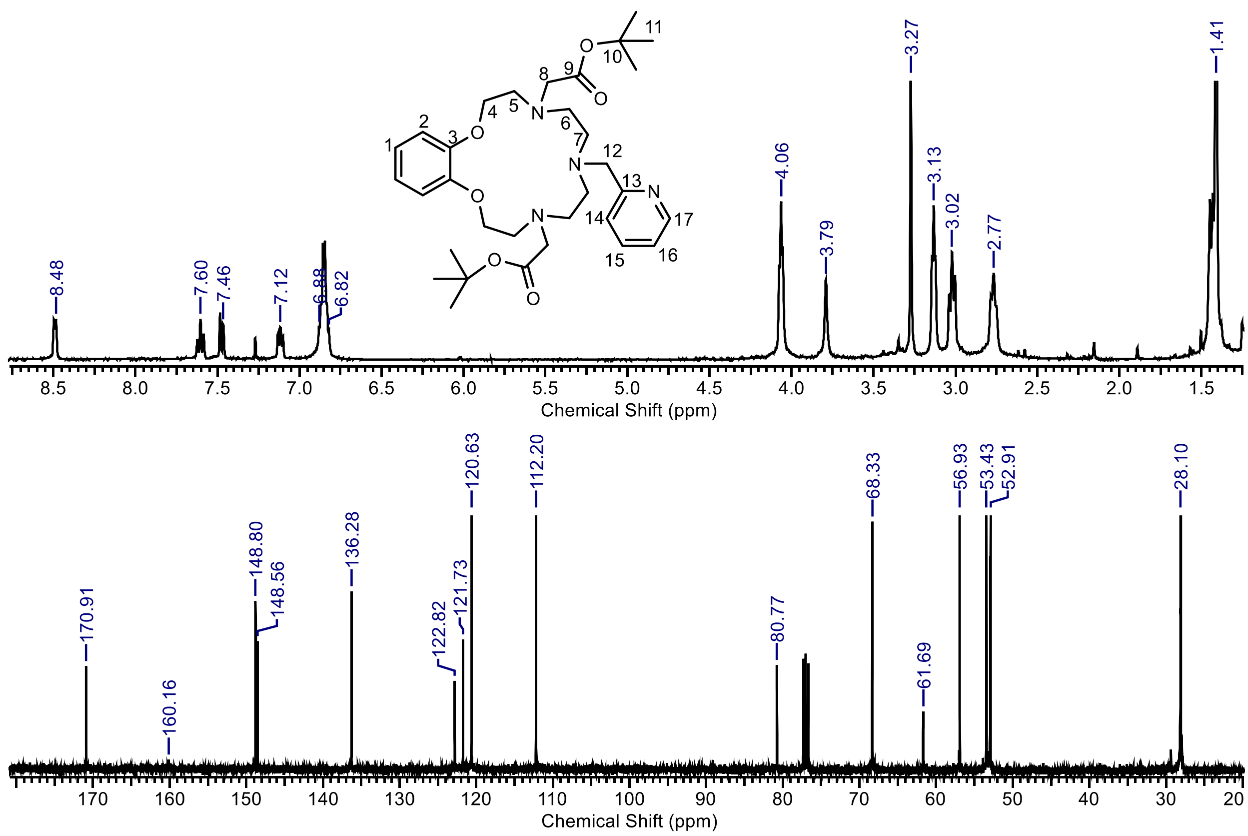

Figure S7. ^{1}H and ^{13}C NMR spectra of 4 in $CDCl_3$.

Figure S8. COSY spectrum of **4** in $CDCl_3$.

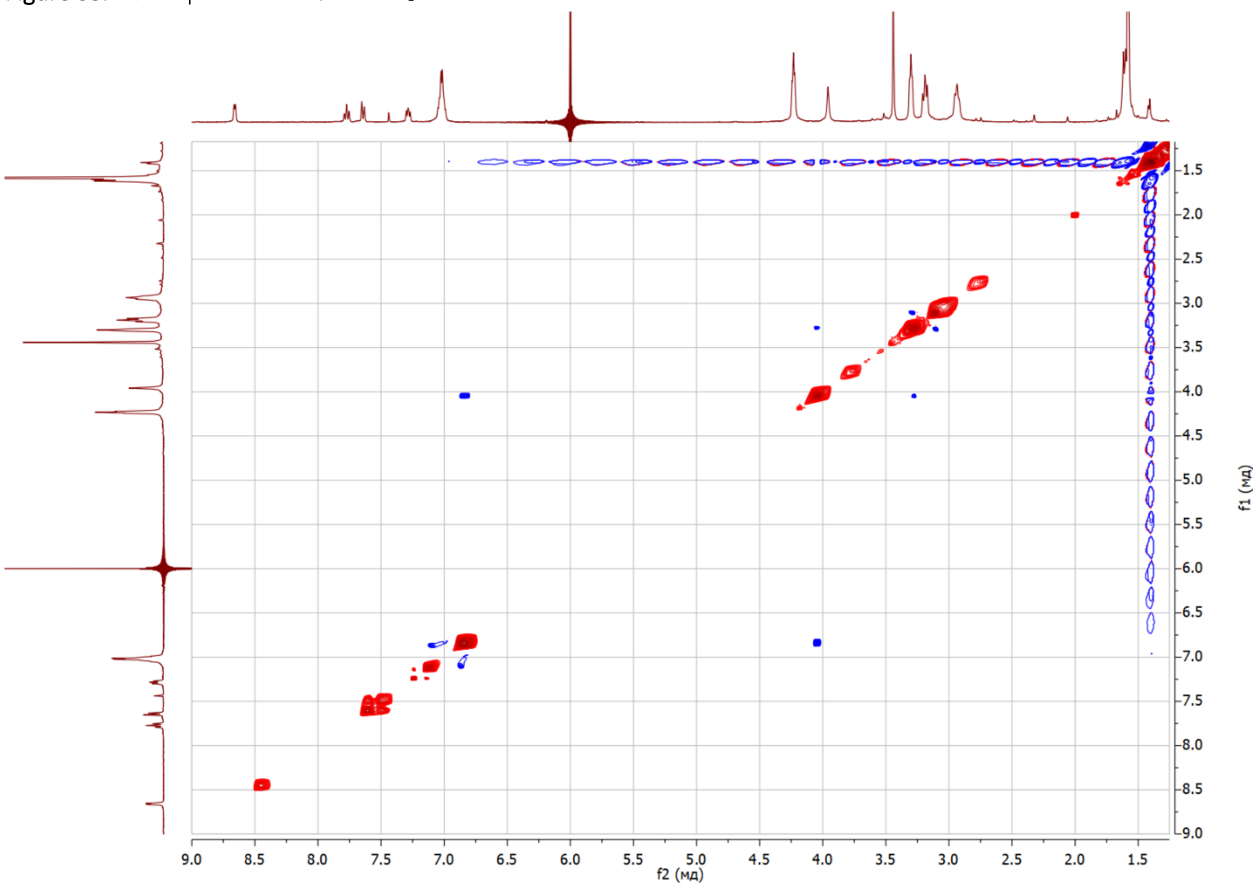

Figure S9. NOESY spectrum of **4** in $CDCl_3$.

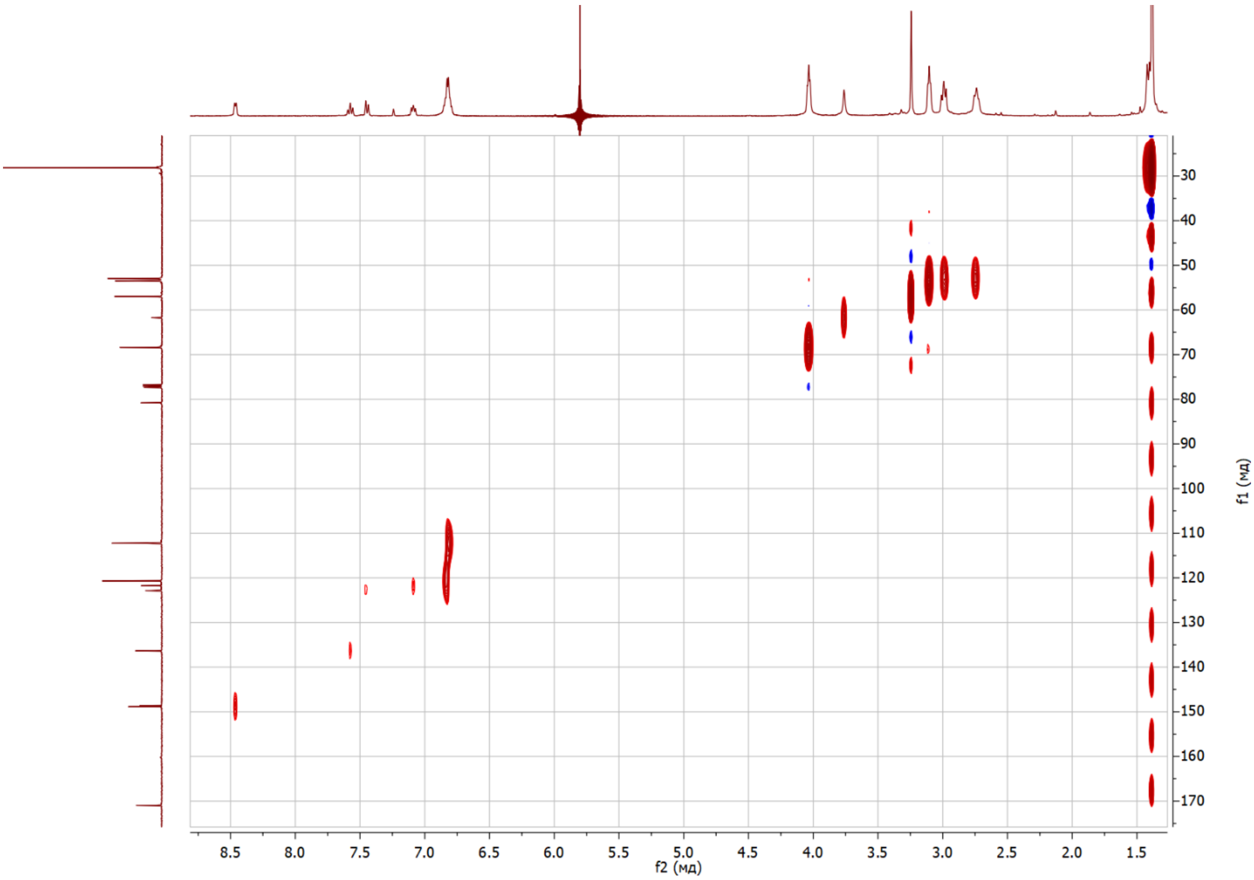

Figure S10. HSQC spectrum of **4** in $CDCl_3$.

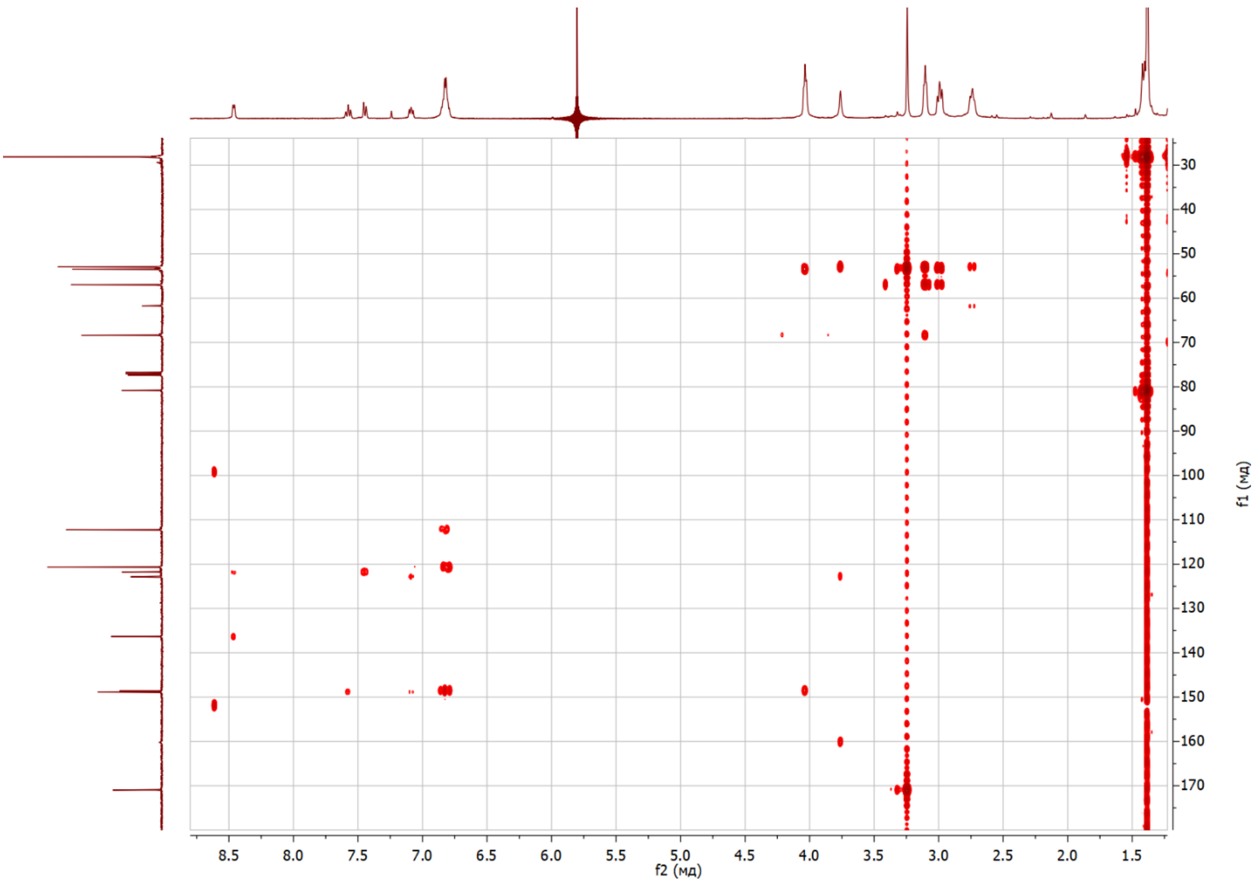

Figure S11. HMBC spectrum of **4** in $CDCl_3$.

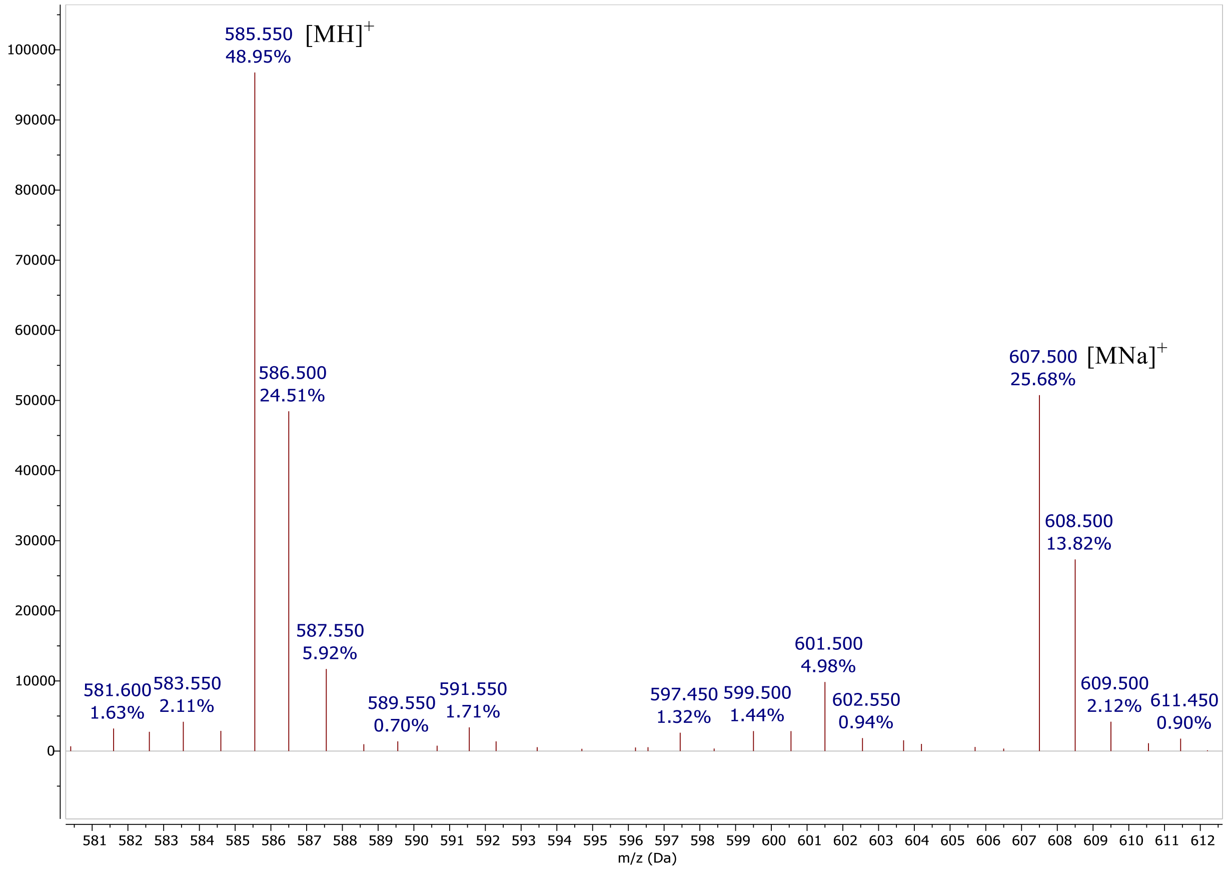

Figure S12. MS (ESI) spectrum of **4**.

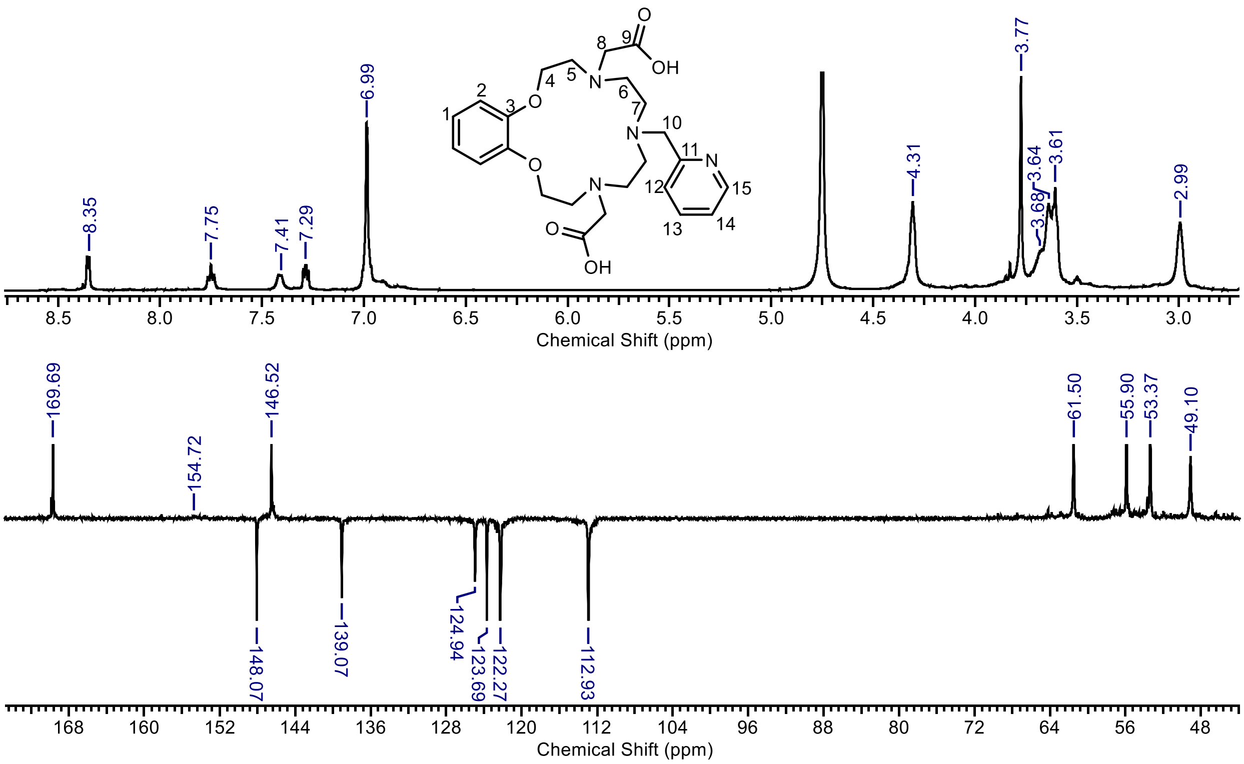

Figure S13. ^{1}H and ^{13}C NMR spectra of **H_2BA2A1Py** in D_2O (pD = 5.7).

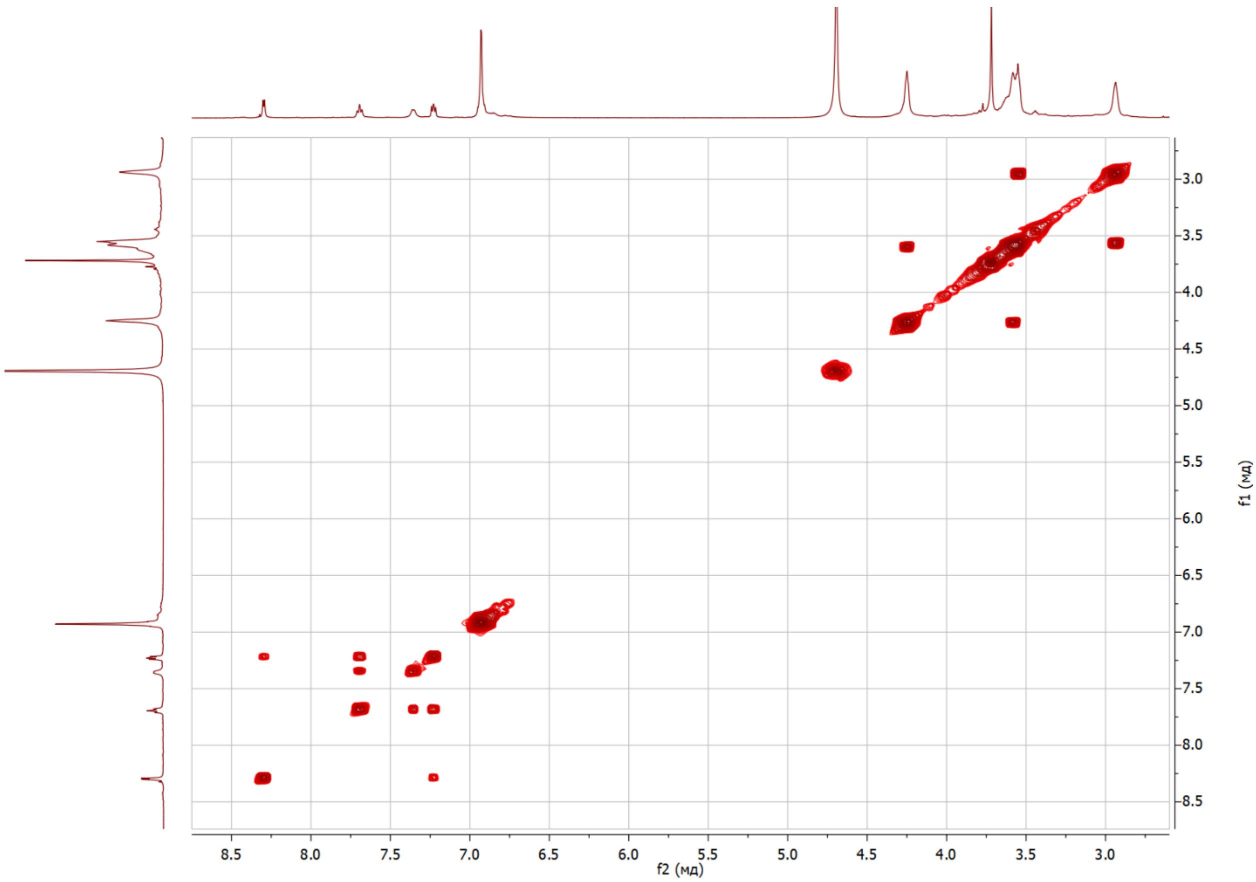

Figure S14. COSY spectrum of **H_2BA2A1Py** in D_2O (pD = 5.7).

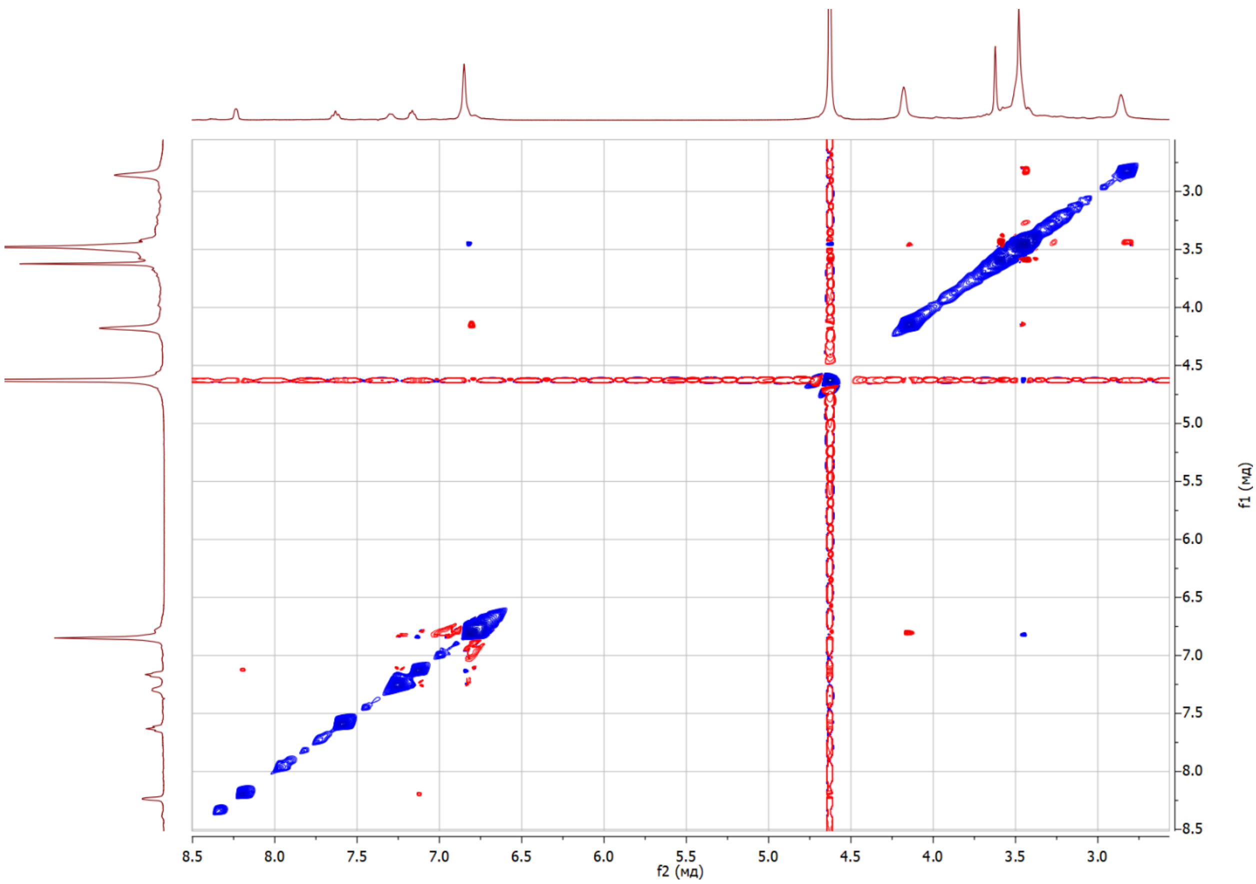

Figure S15. NOESY spectrum of **H_2BA2A1Py** in D_2O (pD = 5.7).

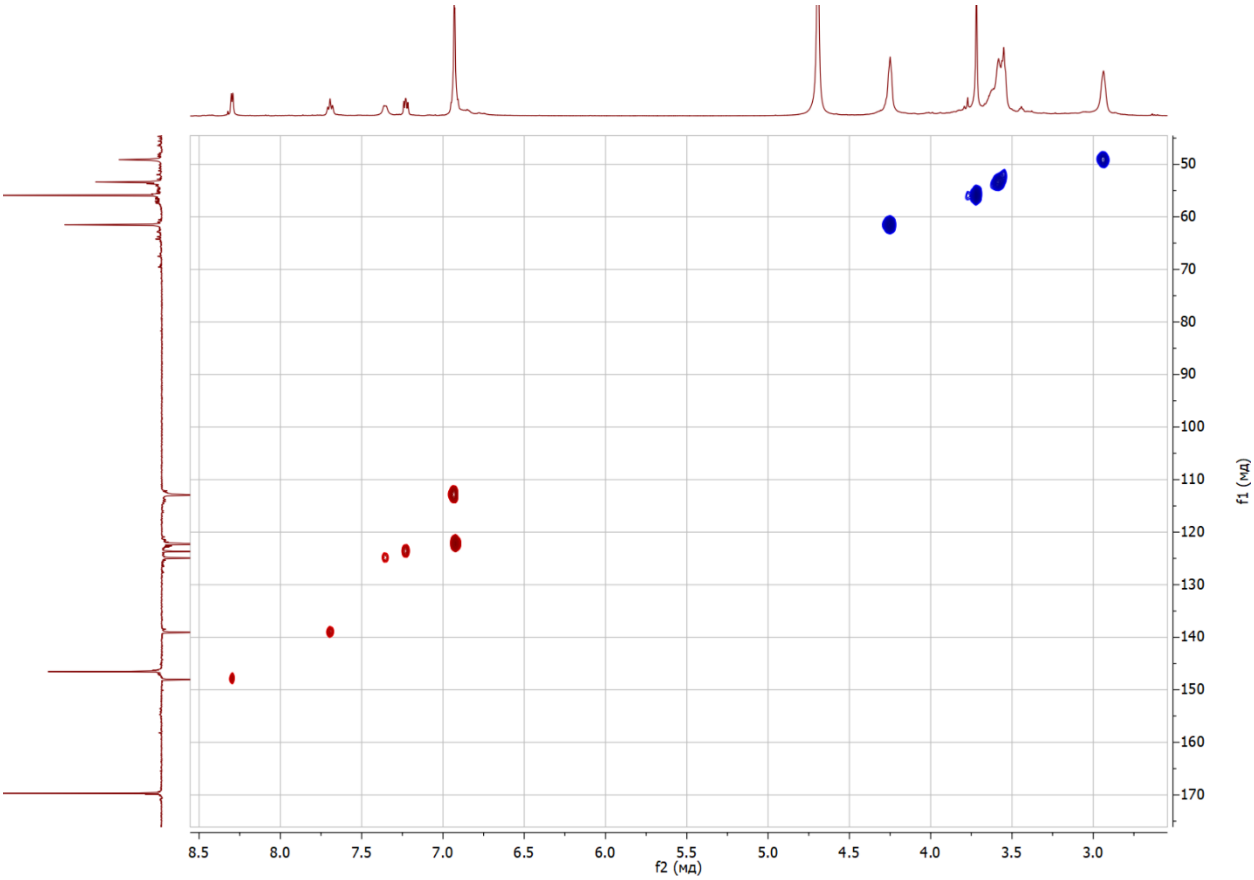

Figure S16. HSQC spectrum of **H_2BA2A1Py** in D_2O (pD = 5.7).

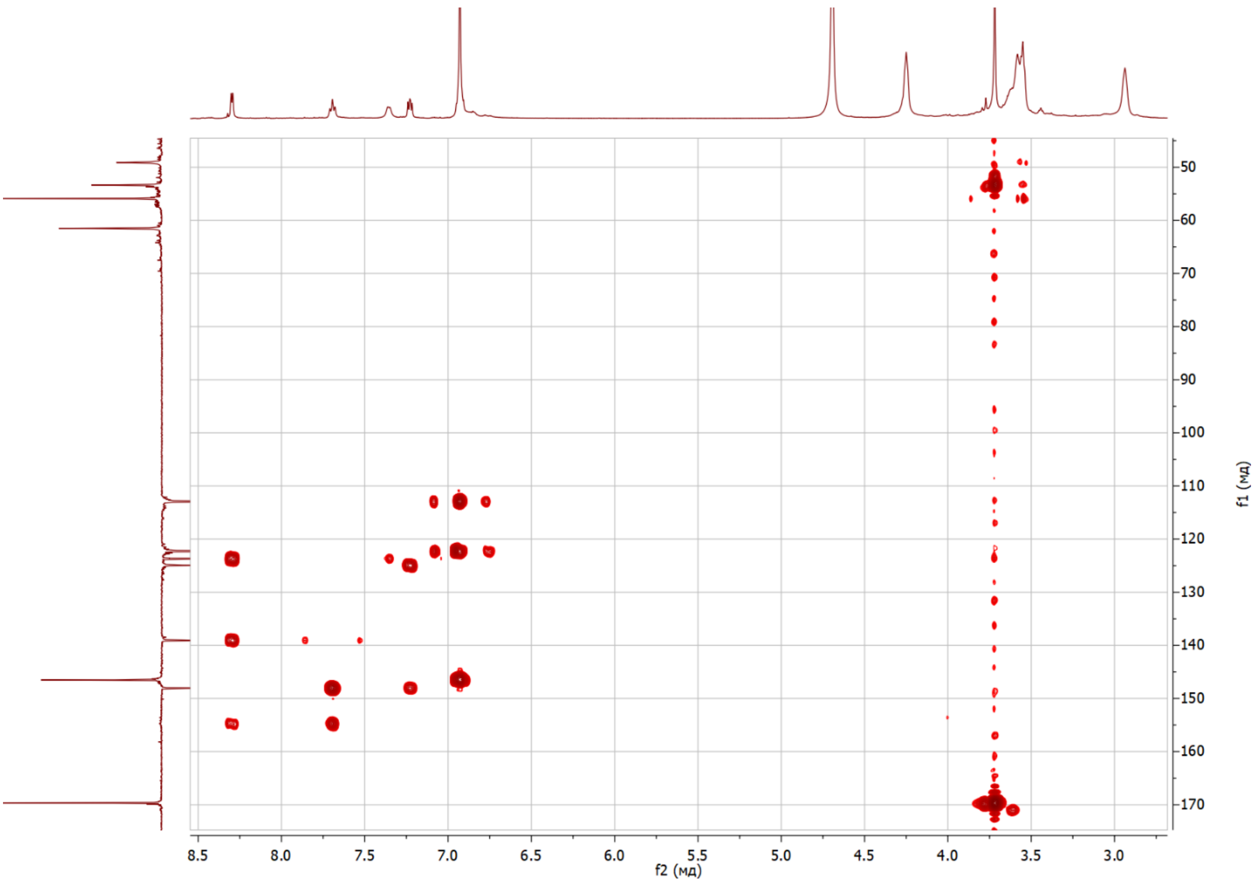

Figure S17. HMBC spectrum of **H_2BA2A1Py** in D_2O (pD = 5.7).

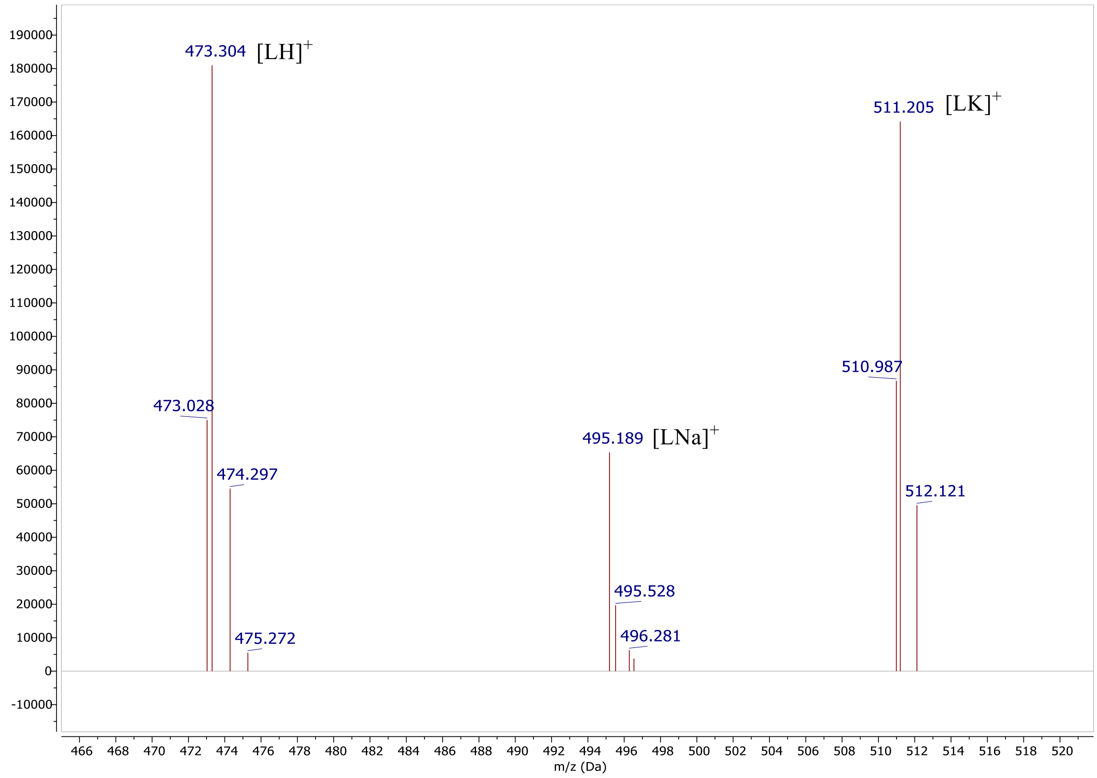

Figure S18. MS (ESI) spectrum of H_2BA2A1Py.

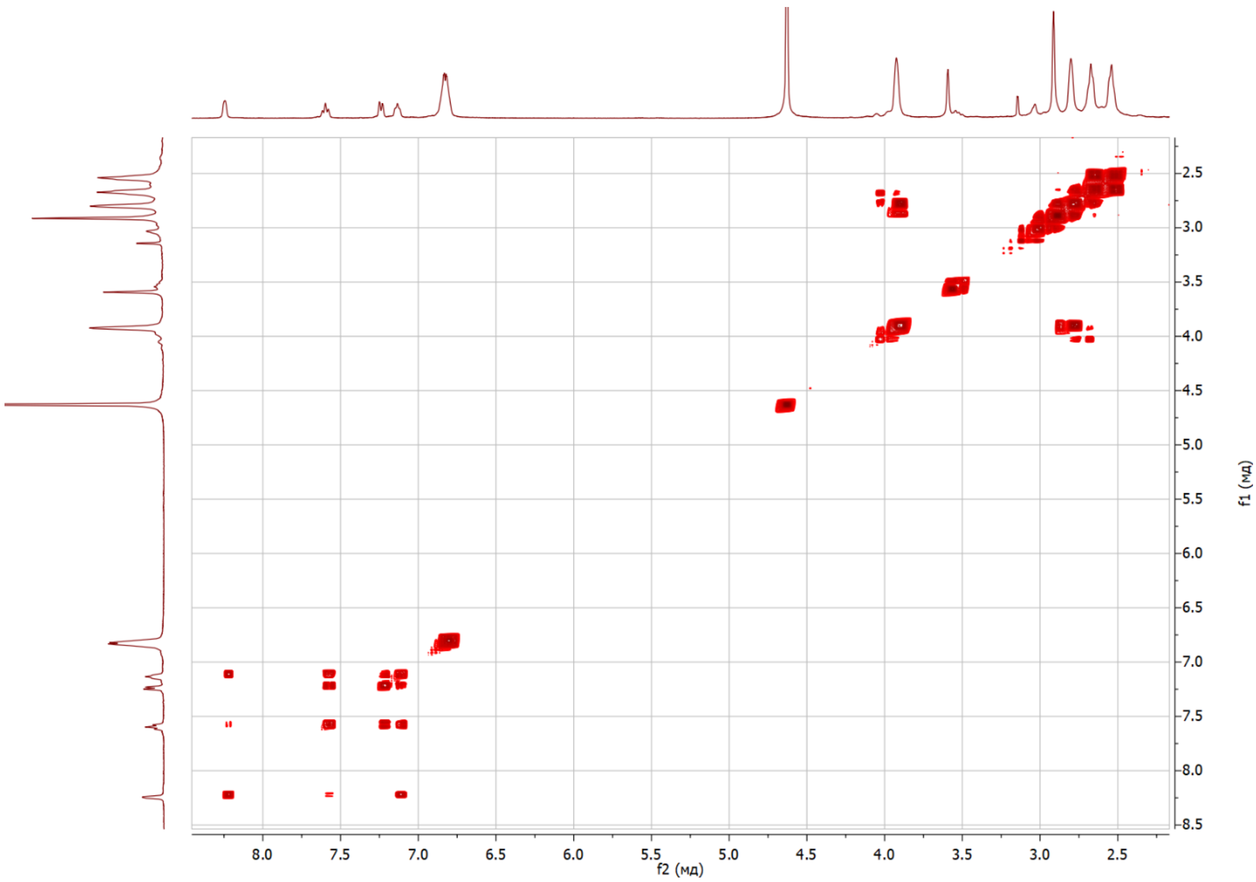

Figure S19. COSY spectrum of BA2A1Py^{2-} in D_2O (pD = 11.2).

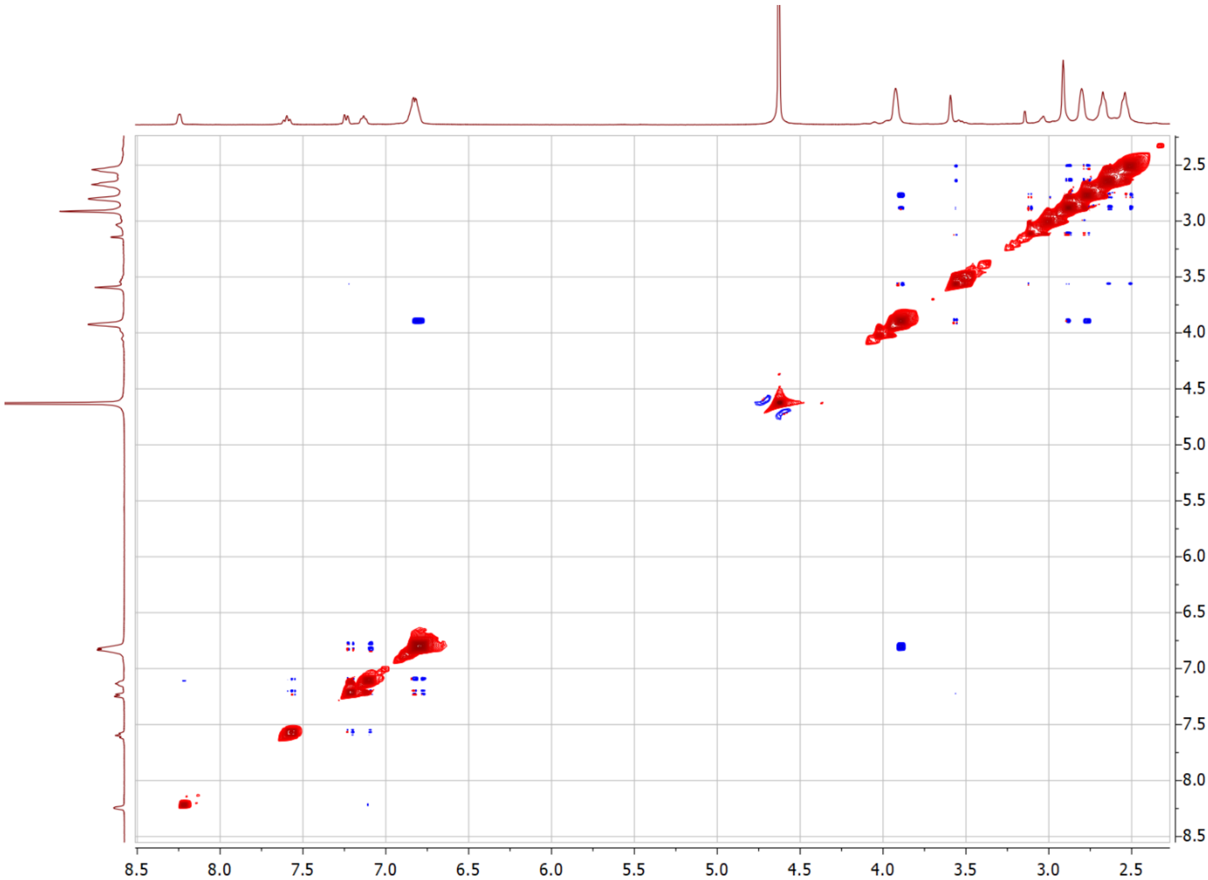

Figure S20. NOESY spectrum of **BA2A1Py**$^{2-}$ in D_2O (pD = 11.2).

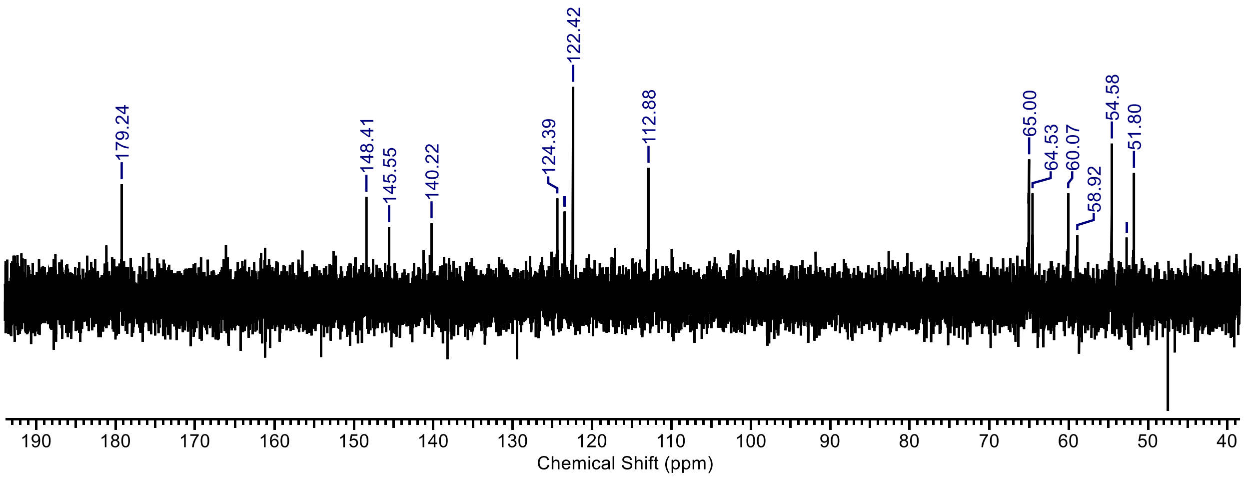

Figure S21. ^{13}C NMR spectrum of **H$_2$BA2A1Py** in the presence of Pb^{2+} (C(L) = 10 мM, pD=6.3) in D_2O.

Table S1. ^{1}H NMR chemical shifts (Δδ, ppm) of **H_2BA2A1Py** recorded in D_2O solution in the absence and presence of Pb^{2+}.

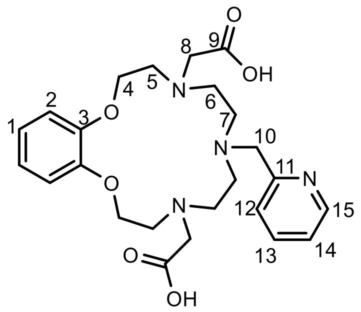

	BA2A1Py^{2-} (pD = 11.2)	**HBA2A1Py$^-$** (pD = 8.5)	**H_2BA2A1Py** (pD = 5.7)	**H_3BA2A1Py$^+$** (pD = 2.6)	Pb·**BA2A1Py** (pD = 6.3)	Pb·**BA2A1PyOH$^-$** (pD = 10.5)	Pb·**HBA2A1Py$^+$** (pD = 2.4)
H_1	6.93	6.97 (Δδ = 0.04)	6.99 (Δδ = 0.06)	7.05 (Δδ = 0.12)	7.06 (Δδ = 0.13)	7.06 (Δδ = 0.13)	7.06 (Δδ = 0.13)
H_2							
H_{4a}	4.03	4.18 (Δδ = 0.15)	4.31 (Δδ = 0.28)	4.40 (Δδ = 0.37)	4.31 (Δδ = 0.28)	4.31 (Δδ = 0.28)	4.32 (Δδ = 0.29)
H_{4e}					4.03 (Δδ = 0)	4.02 (Δδ = -0.01)	4.06 (Δδ = 0.03)
H_{5a}	2.91	3.26 (Δδ = 0.35)	3.64 (Δδ = 0.73)	3.70 (Δδ = 0.79)	2.73 (Δδ = -0.18)	2.71 (Δδ = -0.20)	2.80 (Δδ = -0.11)
H_{5e}					3.23 (Δδ = 0.32)	3.20 (Δδ = 0.29)	3.22 (Δδ = 0.31)
H_{6a}	2.78	3.26 (Δδ = 0.48)	3.61 (Δδ = 0.83)	3.68 (Δδ = 0.90)	3.11 (Δδ = 0.33)	3.10 (Δδ = 0.32)	3.13 (Δδ = 0.35)
H_{6e}					2.70 (Δδ = -0.08)	2.71 (Δδ = -0.07)	2.77 (Δδ = -0.01)
H_{7a}	2.64	3.03 (Δδ = 0.39)	2.99 (Δδ = 0.35)	3.09 (Δδ = 0.45)	3.05 (Δδ = 0.41)	3.04 (Δδ = 0.40)	3.09 (Δδ = 0.45)
H_{7e}					2.54 (Δδ = -0.10)	2.54 (Δδ = -0.10)	2.63 (Δδ = -0.01)
H_{8x}	3.02	3.36 (Δδ = 0.34)	3.77 (Δδ = 0.75)	3.83 (Δδ = 0.81)	3.70 (Δδ = 0.68)	3.69 (Δδ = 0.67)	3.74 (Δδ = 0.72)
H_{8y}					2.27 (Δδ = -0.75)	2.25 (Δδ = -0.77)	2.44 (Δδ = -0.58)
H_{10}	3.70	3.92 (Δδ = 0.22)	3.68 (Δδ = -0.02)	4.12 (Δδ = 0.42)	4.57 (Δδ = 0.87)	4.56 (Δδ = 0.86)	4.60 (Δδ = 0.90)
H_{12}	7.34	7.41 (Δδ = 0.07)	7.41 (Δδ = 0.07)	8.05 (Δδ = 0.71)	7.53 (Δδ = 0.19)	7.53 (Δδ = 0.19)	7.56 (Δδ = 0.22)
H_{13}	7.71	7.70 (Δδ = -0.01)	7.75 (Δδ = 0.04)	8.44 (Δδ = 0.73)	7.97 (Δδ = 0.26)	7.97 (Δδ = 0.26)	8.00 (Δδ = 0.29)
H_{14}	7.24	7.28 (Δδ = 0.04)	7.29 (Δδ = 0.05)	7.90 (Δδ = 0.66)	7.47 (Δδ = 0.23)	7.47 (Δδ = 0.23)	7.51 (Δδ = 0.27)
H_{15}	8.35	8.36 (Δδ = 0.01)	8.35 (Δδ = 0)	8.62 (Δδ = 0.27)	8.38 (Δδ = 0.03)	8.33 (Δδ = -0.02)	8.41 (Δδ = 0.06)

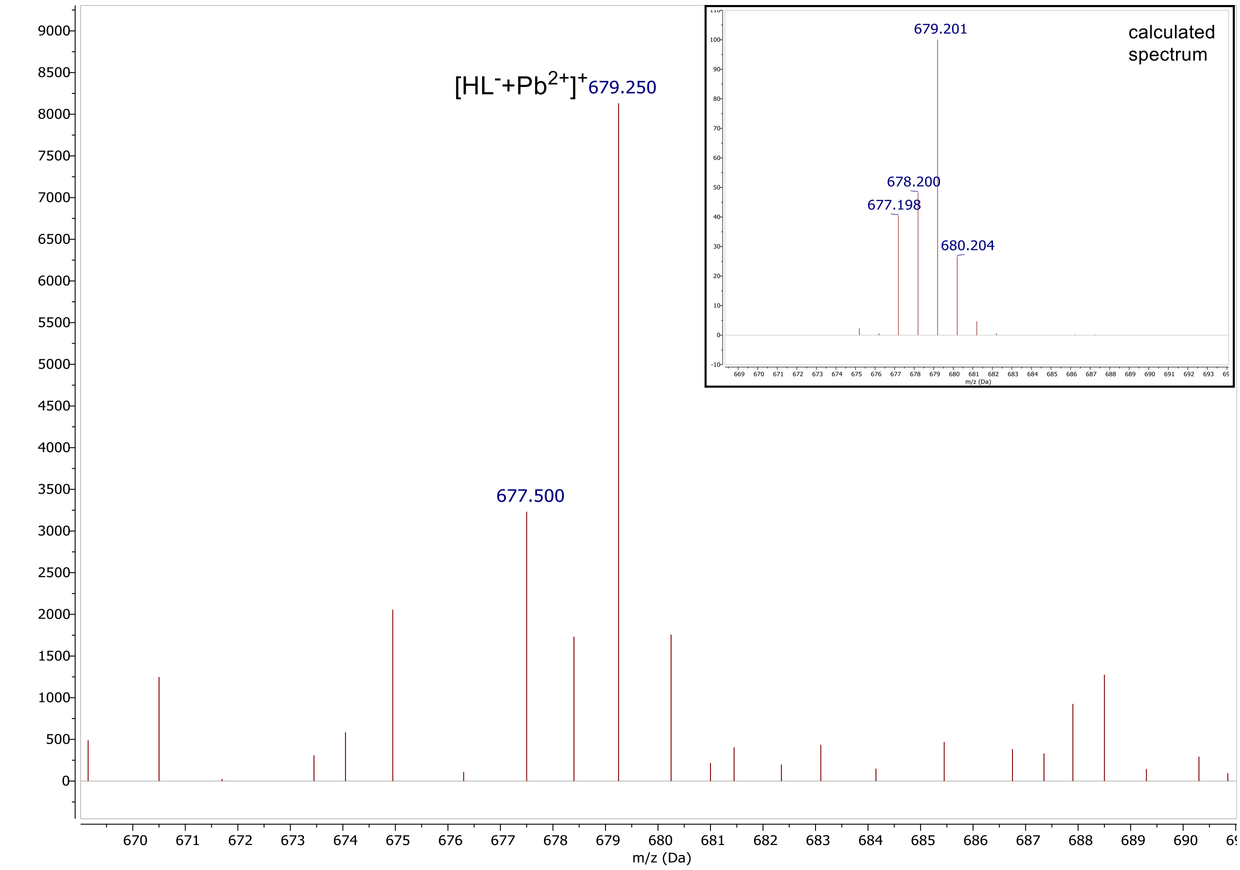

Figure S22. MS (ESI) spectrum of **H_2BA2A1Py** in the presence of Pb^{2+} in water.

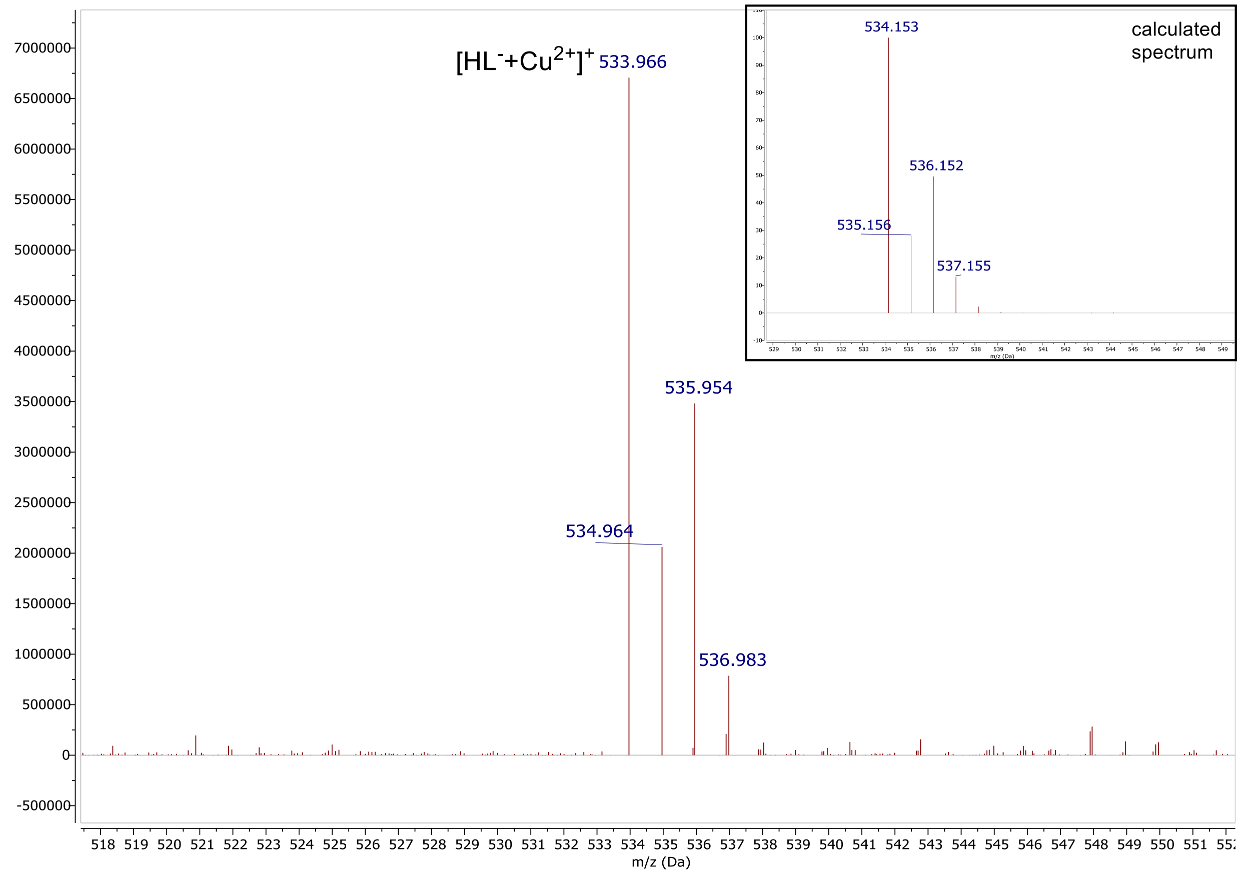

Figure S23. MS (ESI) spectrum of of **H_2BA2A1Py** in the presence of Cu^{2+} in water.

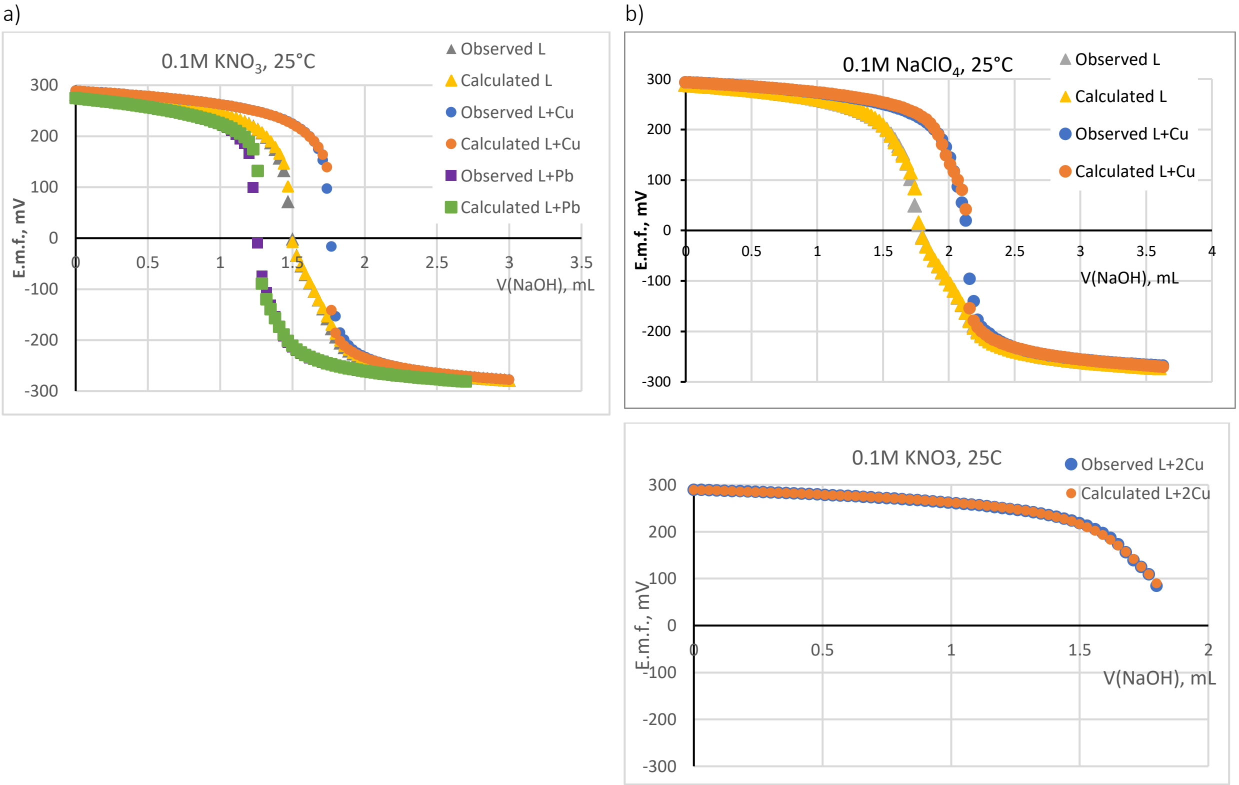

Figure S24. Potentiometric titration curves of solutions, containing 1 mM of L and 1 mM of L with 1 mM of M^{2+} in 0.1 M KNO_3 (a) 0.1M $NaClO_4$ (b) and 1 mM of L with 2 mM of Cu^{2+} in 0.1 M KNO_3.

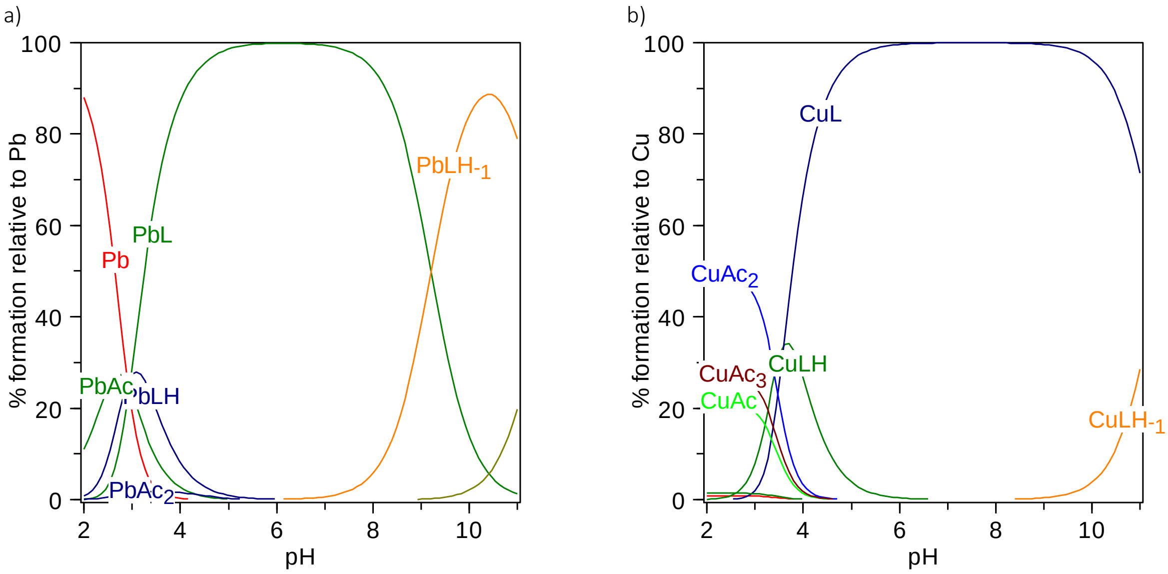

Figure S25. Species distribution diagrams in the systems: a) Pb^{2+} (10 nM), $H_2BA2A1Py$ (0.1mM), Ac^-(0.15 M); b) Cu^{2+} (10 nM), $H_2BA2A1Py$ (0.1mM), Ac^-(0.15 M).

a)

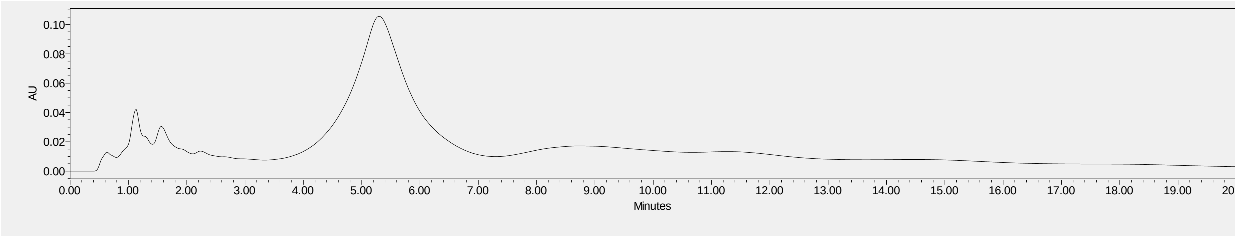

b)

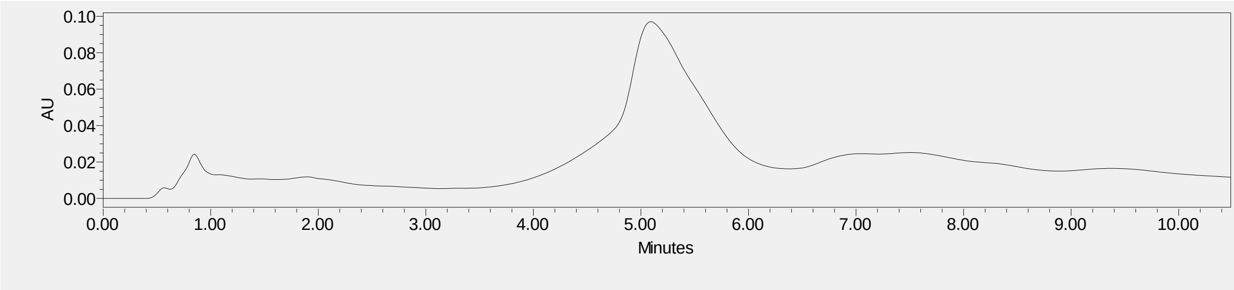

c)

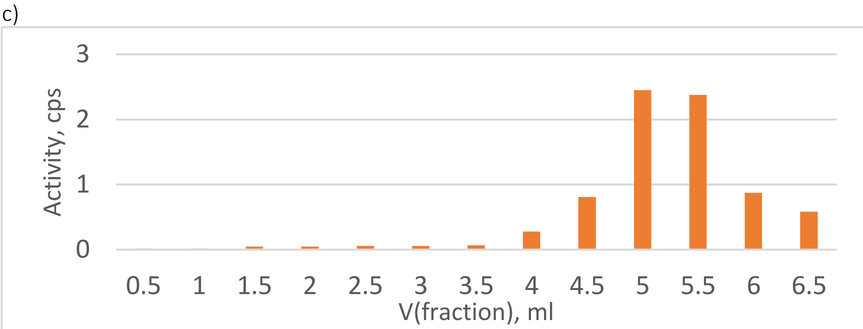

Figure S26. Chromatograms of: a) Cu-BA2A1Py (non-radioactive, 1.7 mM, pH5.3) recorded by UV-Vis detector at 267 nm; b) Pb-BA2A1Py (non-radioactive, 2 mM, pH7.4) recorded by UV-Vis detector at 267 nm; c) [^{210}Pb]Pb-BA2A1Py (radioactive, c(L) = 0.1mM, pH5.3, without NaOAc) plotted according to measured activity in the collected fractions (correction to dead volume was applied).

a)

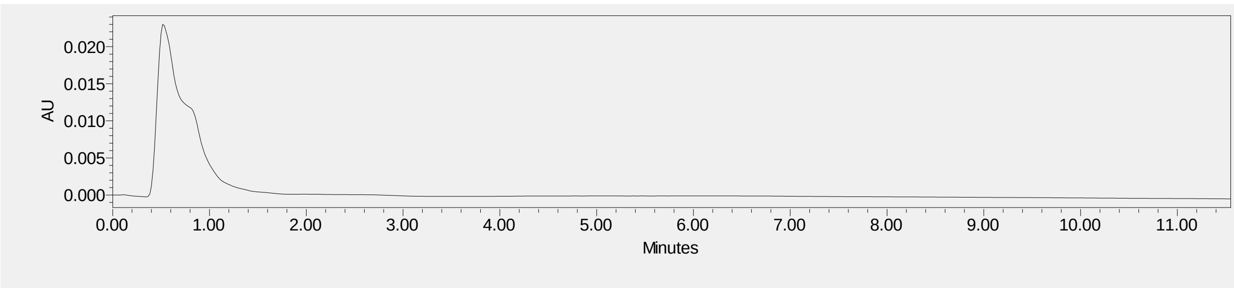

b)

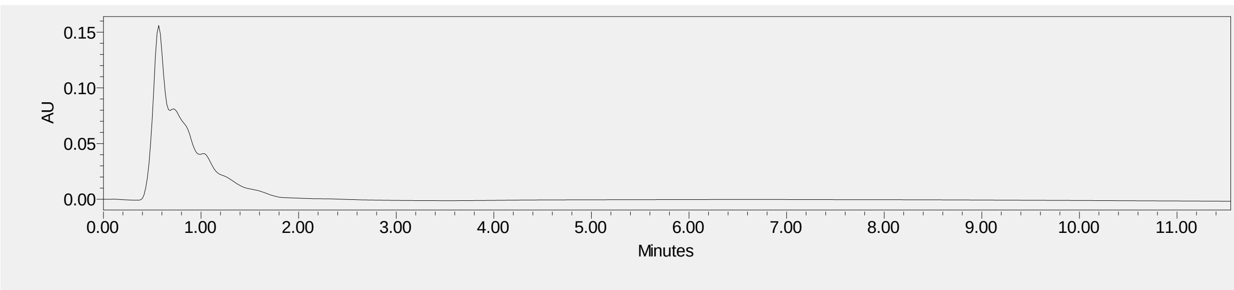

Figure S27. Chromatogram of AcONa (0.15M) recorded by UV-Vis detector at 221 nm (a) and 267 nm (b), in the mode used for Pb-BA2A1Py complex (isocratic, H_2O – 0.9, CH_3CN – 0.1).